available at www.sciencedirect.com

ScienceDirect

www.elsevier.com/locate/brainres

BRAIN RESEARCH

Research Report

Group independent component analysis reveals consistent resting-state networks across multiple sessions

Sharon Chen[a,d,1], Thomas J. Ross[a,1], Wang Zhan[a], Carol S. Myers[b], Keh-Shih Chuang[c], Stephen J. Heishman[b], Elliot A. Stein[a], Yihong Yang[a,*]

[a]Neuroimaging Research Branch, National Institute on Drug Abuse, NIH, 251 Bayview Boulevard, Suite 200, Baltimore, MD 21224, USA
[b]Clinical Pharmacology and Therapeutics Branch, National Institute on Drug Abuse, NIH, Baltimore, MD 21224, USA
[c]Department of Biomedical Engineering and Enviromental Sciences, National Tsing-Hua University, Hsin Chu, Taiwan
[d]Faculty of Medical Radiology, Kaohsiung Medical University, Kaohsiung, Taiwan

ARTICLE INFO

Article history:
Accepted 10 August 2008
Available online 18 August 2008

Keywords:
Default-mode
Dimensionality
fMRI
Longitudinal studies

ABSTRACT

Group independent component analysis (gICA) was performed on resting-state data from 14 healthy subjects scanned on 5 fMRI scan sessions across 16 days. The data were reduced and aggregated in 3 steps using Principal Components Analysis (PCA, within scan, within session and across session) and subjected to gICA procedures. The amount of reduction was estimated by an improved method that utilizes a first-order autoregressive fitting technique to the PCA spectrum. Analyses were performed using all sessions in order to maximize sensitivity and alleviate the problem of component identification across session. Across-session consistency was examined by three methods, all using back-reconstruction of the single-session or single-subject/session maps from the grand (5-session) maps. The gICA analysis produced 55 spatially independent maps. Obvious artifactual maps were eliminated and the remainder were grouped based upon physiological recognizability. Biologically relevant component maps were found, including sensory, motor and a 'default-mode' map. All analysis methods showed that components were remarkably consistent across session. Critically, the components with the most obvious physiological relevance were the most consistent. The consistency of these maps suggests that, at least over a period of several weeks, these networks would be useful to follow longitudinal treatment-related manipulations.

Published by Elsevier B.V.

1. Introduction

Intrinsic non-directed brain activity has been investigated using spontaneous fluctuations in resting-state functional magnetic resonance imaging (fMRI) signal (Biswal et al., 1995). Brain connectivity maps in the absence of task performance have been reported to follow specific brain circuits, including sensorimotor, visual, auditory, and language processing networks (Biswal et al., 1995; Lowe et al., 1998; Xiong et al., 1999; Cordes et al., 2000; Greicius et al., 2003; Beckmann et al., 2005; Fox et al., 2005). Among these observations, the existence of a brain network including posterior cingulate cortex (PCC) and medial prefrontal cortex (MPF) has been reported (Fox et al., 2005; Greicius et al., 2003), which supports previous sugges-

* *Corresponding author*. Fax: +1 443 740 2816.
E-mail address: yihongyang@intra.nida.nih.gov (Y. Yang).
Abbreviations: gICA, group Independent Components Analysis; PR, Physiological Recognizability
[1] Authors contributed equally.

0006-8993/$ – see front matter. Published by Elsevier B.V.
doi:10.1016/j.brainres.2008.08.028

tions that there is a functionally significant default brain mode in the awake resting-state (Gusnard and Raichle, 2001; Raichle et al., 2001). Since the brain expends a considerable amount of energy for neuronal signaling processes in the absence of a particular task (Shulman et al., 2004; Sibson et al., 1998), it is further argued that, in pursuit of better understanding of brain functions, observation of intrinsic brain activity may be at least as important as that of evoked activity (Raichle and Gusnard, 2005). Recently, various applications of resting-state fMRI have been demonstrated, including studies of Alzheimer's disease (Greicius et al., 2003; Li et al., 2002), schizophrenia (Liang et al., 2006), epilepsy (Waites et al., 2006), cocaine dependence (Li et al., 2002) and antidepressant effects (Anand et al., 2005).

With growing interest in resting brain activity, it becomes increasingly important to fully understand and characterize this intrinsic brain function. Consistency (or repeatability) of resting-state activity along time and across subjects is crucial for longitudinal and group studies, but has not been well studied. The degree of temporal consistency, for example, is essential for assessing changes of resting-state brain functions over a period of time, such as monitoring disease-related, therapeutic or drug-withdrawal effects. Although repeatability of task-induced brain activation in multi-session data sets has been investigated (Marshall et al., 2004; McGonigle et al., 2000), analysis of consistency of resting-state data is challenging due to the lack of synchronization in resting time courses across sessions or subjects.

Independent component analysis (ICA), a multivariate data-driven method (Bell and Sejnowski, 1995; Comon, 1994), has been used to reveal task-induced brain activation (Calhoun et al., 2001; McKeown et al., 1998) and recently resting-state brain networks (Beckmann et al., 2005) without a priori knowledge about the pattern of the fMRI time course. This technique has recently been used to investigate the consistency of resting-state networks across two imaging sessions (Damoiseaux et al., 2006). In this study, we used group-level ICA to assess the repeatability of intrinsic brain activity across 5 sessions (within 16 days) and across 14 subjects. We identified brain networks from the resting-state data and quantified the consistency using three metrics. Results of this study provide a "baseline" for longitudinal group studies using resting-state fMRI, at least over this timeframe.

2. Results

Two methods were used to combine the data across subjects and sessions (see Experimental procedures). The results presented herein are from the first method of concatenation ($gICA_1$), combining across subjects then sessions; $gICA_2$ produced extremely similar results (not shown).

2.1. *Physiologically recognizable component maps*

Resting-state data from 14 subjects scanned on five separate scan sessions were analyzed with group ICA, yielding 55 components. Of the 55 component maps, 9 consistent maps relevant to physiological functions (PR1) were identified, based on known neuroanatomical circuits/systems. These component maps are shown in Fig. 1 and include: a) medial occipital cortices, b) bilateral temporal cortices and anterior cingulate cortex (ACC), c) PCC, ACC, and bilateral inferior parietal cortex, d) bilateral motor regions, e) right medial and lateral frontal cortices and parietal cortex, f) left medial and lateral frontal cortices and parietal cortex, g) cerebellum, h) medial frontal/ACC, bilateral dorsolateral prefrontal cortex (DLPFC), bilateral temporal cortex and striatum and i) bilateral lateral occipital cortices. The component map (c), is often described as the 'default-mode' brain network (Gusnard and Raichle, 2001). Additional maps were ascribed to being likely physiologically recognizable (PR2, $n=7$) and possibly physiologically recognizable (PR3, $n=8$). The majority of the maps, 31, were deemed to be artifactual or noise-based (PR4). Maps from groups PR2–PR4 are shown in the Supplemental materials.

2.2. *Consistency of the component maps across sessions*

The correlation coefficients (CC) between the five group ICs at each session and the corresponding grand IC, consisting of data from all 5 sessions, were calculated, averaged and ranked by their mean CC values and are presented in Fig. 2a. All ICs show remarkable consistency, with correlations ranging between 0.5 and 0.93. Non-parametric analysis indicates that the 4 groups differ in their average correlation (Kruskal–Wallis $H=10.7$, $p<0.014$). Group PR1 (average rank=40.7) showed higher correlation than the non-physiologically recognizable group PR4 (average rank=24.5) based upon post-hoc tests (Mann–Whitney $U=54$, $p<0.006$). Groups PR2 and PR3 (average ranks=19.3 and 34.9, respectively) did not differ from PR4.

The results from a voxel-wise ANOVA, used to assess statistically significant changes in component weights across session, are presented in Fig. 2b. For the most interesting (PR1), and usually most consistent, components fewer than 20% of the voxels showed a main effect of session at a threshold of $p<0.1$. At this threshold, one would expect 10% of the voxels to have a session effect by chance alone (type I error). For the noise components (PR4), 20–40% of the voxels had a session effect at this threshold. The results are analogous for the more stringent thresholds of $p<0.05$ and $p<0.01$ (i.e. about twice the expected false-positive rate for the most consistent components).

Spatial overlap maps, used to assess repeatability of thresholded maps, are presented in Fig. 3. In general, there is excellent overlap between all five sessions and the grand map. Unsurprisingly, there is nearly perfect overlap in the components that had the highest average correlation; see Figs. 3a–c. However, as the component number increases (i.e. decreasing average correlation), regions present in the grand map, but not all sessions, begin to appear. An example is the right frontal region in Fig. 3d. Nonetheless, much of this region was present in 3 of the 5 sessions. Conversely, there are several (small) regions in Fig. 3h that were present in the grand map but exist in fewer than 3 of the single-session maps.

3. Discussion

Group independent components analysis was performed on resting-state fMRI data collected in 5 sessions over the course

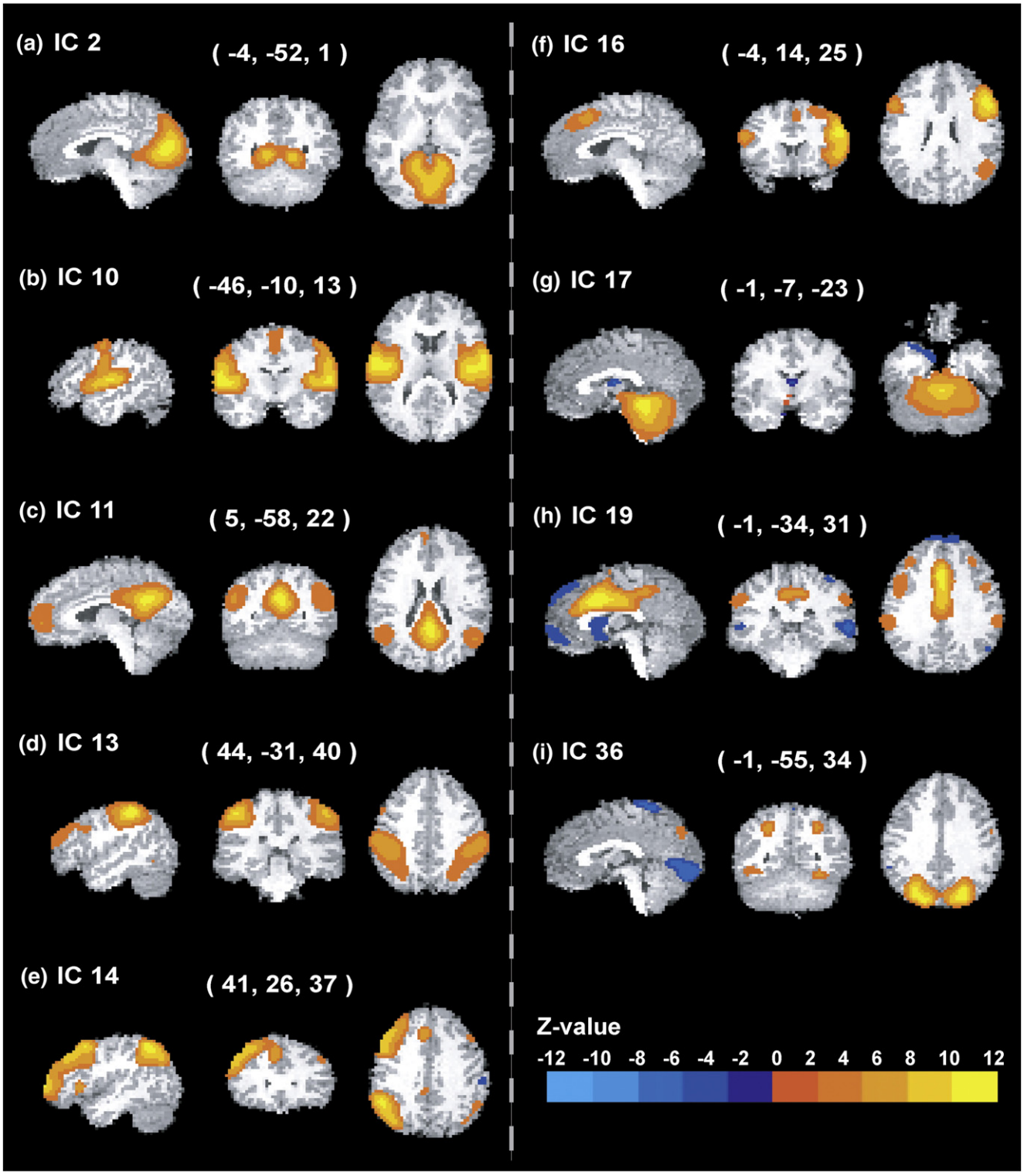

Fig. 1 – Group independent maps for components that were the most physiologically recognizable. The component numbering is consistent with Fig. 2. The numbers in parenthesis represent the distance in mm from the anterior commissure of the sagittal, coronal and axial slices respectively. Z-scores are derived by comparing the voxel's component weight to the mean over space. Regions in blue indicate negative component weights, i.e. opposite temporal pattern to regions in orange/yellow.

of 16 days. We used the noise characteristics of the eigenvalue spectrum to guide three data reduction steps (single scan, single subject across sessions and whole group), ultimately resulting in 55 components. These components include a number of readily-identified neuroanatomical networks and a large number of networks whose physiological significance is

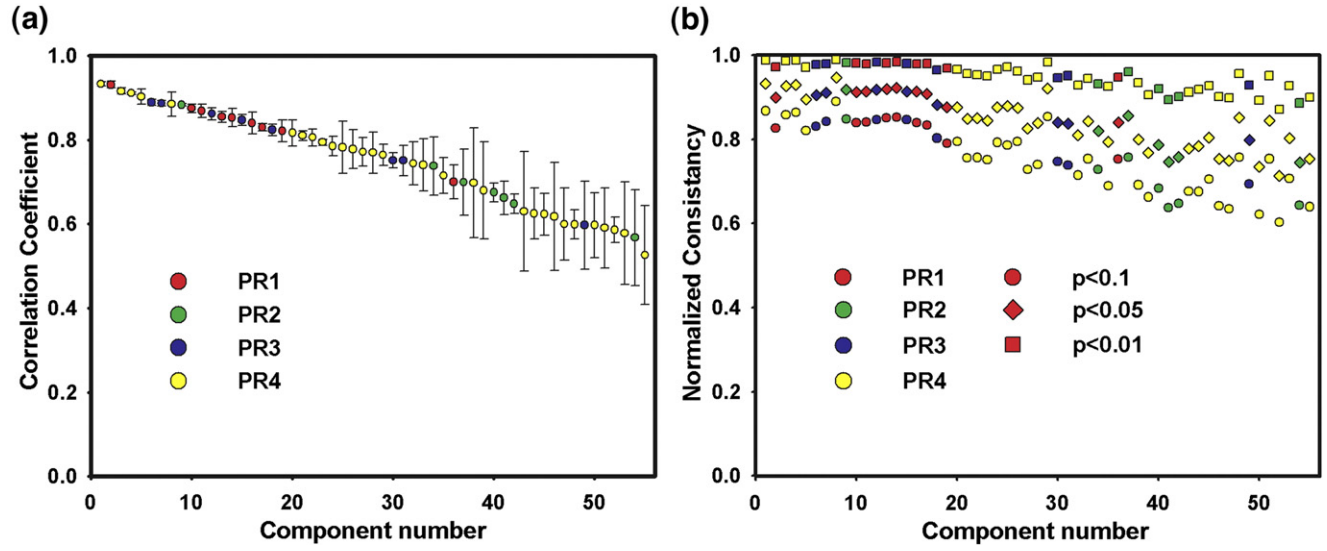

Fig. 2 – (a) Average correlation coefficient across space of the five sessions with the grand map. Error bars indicate standard deviation. (b) Consistency of the component maps as indicated by voxel-wise ANOVA at various thresholds (uncorrected for multiple comparisons). The vertical axis indicates the fraction of voxels without a session effect. Colors indicate group and symbol shapes indicate threshold. Given that the component numbering from ICA is arbitrary, the components were order by correlation coefficient; this same ordering is used throughout the results. PR1–PR4 indicates the ranked physiological recognizability of the components.

much less clear. The bulk of the components appear to be artifactual in nature, driven by eye motion, head motion, or CSF pulsations. However, all components, even those that appear to be noise driven, were remarkably stable across time. Three different methods were used to quantify aspects of the temporal stability, all yielding similar results. Given the number of subjects and sessions that went into this analysis, we believe that the resulting maps represent the most accurate characterization of resting-state networks to date.

The networks identified as physiologically recognizable include: bilateral visual, auditory and motor cortices; individually-lateralized left and right parietal, MPFC and DLPFC; and PCC, ACC, and bilateral inferior parietal cortex. It is perhaps unsurprising that the most consistent of these are the sensory/motor networks. Predicated on the assumption that the networks uncovered in resting-state analysis are those that have developed preferential connections by repeated use, basic sensory and motor functions are in near-constant use during wakefulness and thus should be strongly intraconnected. However, the consistency of the last of the regions listed above, often referred to as the 'default-mode' network (Gusnard and Raichle, 2001; Raichle et al., 2001), is a bit more surprising. These regions are hypothesized to be normally active during unconstrained thinking and suppressed during directed tasks, resulting in task-induced deactivations (McKiernan et al., 2003). On the other hand, resting-state analysis has revealed this network in sleep, the anesthetized state and coma (Boly et al., 2008), thus indicating that the role of this network transcends the conscious state. So, while the exact role of this network is still under debate, the ubiquity of its observation in both tasks and rest make its consistency less surprising. The parietal–DLPFC network is one frequently seen with cognitive tasks involving executive functions and likely represents attentional modulation of these systems (Raz and Buhle, 2006). Attention is a key characteristic of normal cognitive functions, given that attentional modulation is important from the lowest sensory levels (e.g. V1 of the visual system) up through higher cognitive processing. Thus it would be anticipated that these regions would form a consistent network. However, these networks are usually seen bilaterally with cognitive tasks, whereas in our data the left and right networks formed their own components, likely a function of the number of components in our analysis.

The number of components depended upon the PCA data reduction steps. Having a higher number of components would split the interesting components into several subcomponents. Conversely, a low number of components would merge components together. Anecdotally, when we reduced the number of components to 30, the attention networks merged, yielding bilateral DLPFC and parietal regions in a single component. Our choice of the number of included components was motivated by an estimation of the amount of information in the data. By further reducing the number of components, separate but similar components will combine. Nonetheless, others have found lateralized results similar to those presented here (Damoiseaux et al., 2006). Thus, while it is likely that there is similarity between spontaneous activity in parietal and contralateral parietal cortices, each is just more similar to ipsilateral DLPFC than to its homologous cortex.

The components identified as appearing physiologically recognizable agree fairly well with results in the literature using similar methods. For example, Damoiseaux et al. (2006) subjectively selected 10 component maps (out of 25) by visual inspection. Of those, 7 appear to be extremely similar to those in our PR1 group, including primary motor, visual and auditory

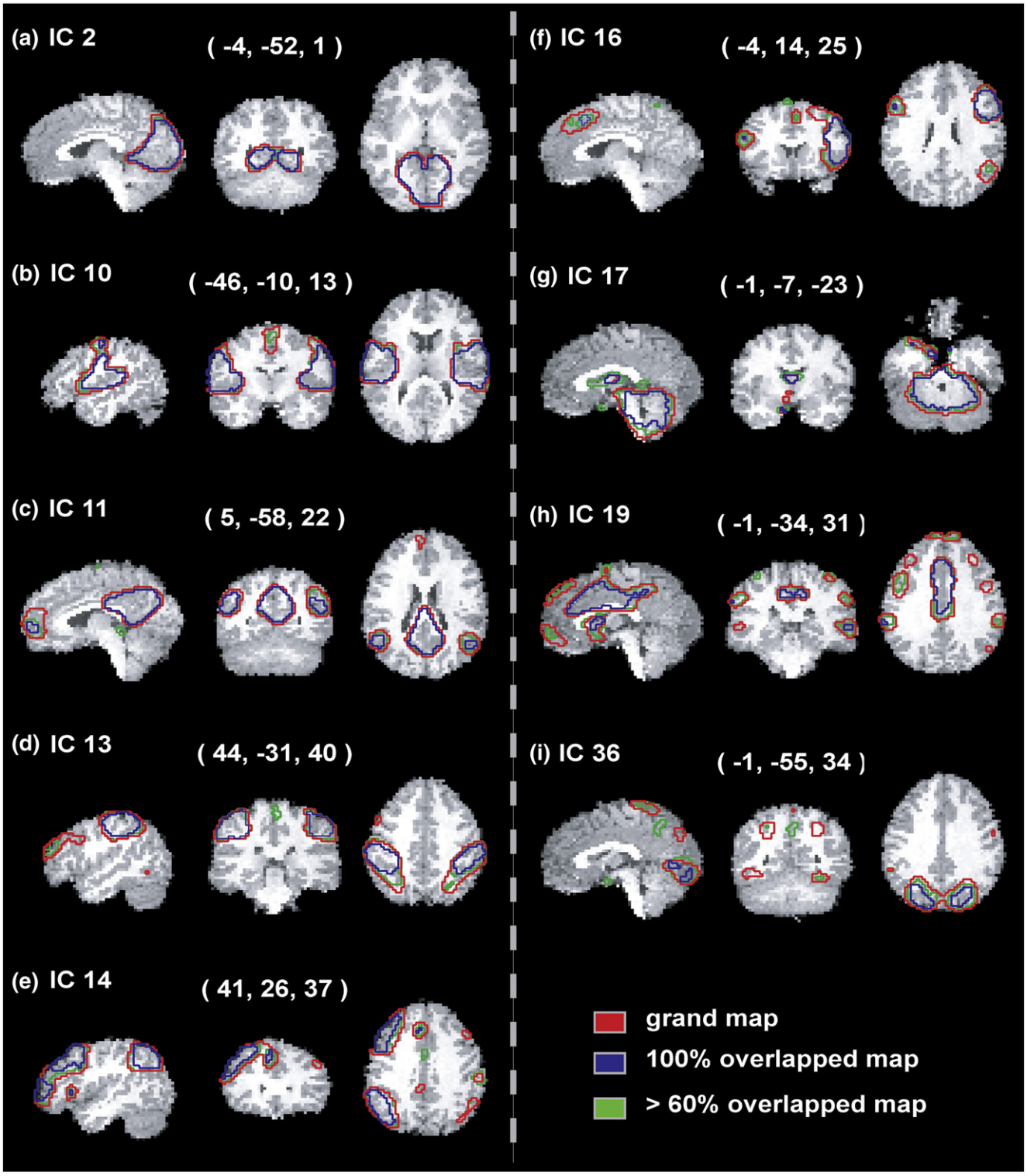

Fig. 3 – Overlap of the grand (5-session) maps with the single-session maps. For clarity, outlines of the regions are presented. Regions in red were in the grand map (identical to Fig. 1), blue were in all 5 single-session maps and green were in at least 3 of the 5 single-session maps. See Fig. 1 for the labeling.

cortices, left- and right-lateralized frontoparietal networks and the 'default-mode' network. In contrast, Fukunaga et al. (2006) identified about 60% (of about 80 components/subject) as having apparent functional relevance. However, their study included sleeping subjects over a long (40 min) scan, possibly accounting for their lower rate of 'artifactual' components. Furthermore, the networks we found agree well with those seen in sensorimotor, visual, auditory and 'default-mode'

regions identified using seed-voxel based methods (Biswal et al., 1995; Lowe et al., 1998; Xiong et al., 1999; Cordes et al., 2000; Greicius et al., 2003; Fox et al., 2005). This consistency across time and studies seems to indicate that these brain networks are, if not the most important networks, certainly those with the greatest coherence of activation (at least as measured by BOLD) and greatest signal/noise. It would be interesting to see if a disruption in one or more of them are concomitant with a neurological or psychiatric disease.

The most important finding in this study is the remarkable consistency of the networks identified in resting-state data across multiple session and subjects. Previous studies have demonstrated consistency of some resting-state networks using seed-based methods. For example, using a data-driven method (ICA) to choose the seed points, van de Ven et al. (2004) found spatial correlations in networks similar to those presented herein ranging from 0.2 to 0.83 between two sessions in auditory, visual and motor cortices as well as networks derived from parietal seed points. Furthermore, resting-state networks appear to be little changed by an intervening cognitive task in the course of a single scan session (Waites et al., 2005).

The evidence in our work strongly suggests that a single session is sufficient to represent the group-level map. The strongest support is provided by the correlation between the individual session maps and the grand maps. The average correlation ranged from 0.5 to 0.95 and was typically toward the higher end of the range for the most interesting components. The consistency was further supported by the overlap maps, which showed that for most regions all 5 single-session maps passed threshold in the same regions as the grand map. Nevertheless, there were some regions present in the grand map that were not present in all five (or even 3 of 5 in some cases) sessions. These are probably regions that are present to some degree in most sessions, but only strongly in one or two sessions; i.e. a threshold effect. What is not shown in Fig. 3 are regions active for one session only — presumably a much greater set of regions. An obvious explanation for extraneous regions is a noisier map due to impoverished data compared to the grand map; however, there is a more interesting alternative. It is possible that the grand component maps represent regions preferentially biased to communicate. However, these regions are likely interconnected with other brain regions; regions that may be more labile to situational context. Hence, regions identified in single-session (or fewer than five-session) data could represent specific activity, for that session, overlaid on the 'background' activity typical of regions that comprise that component.

The overlap of the single-session data does not tell the whole story. It is possible to have large, significant, amplitude variations in regions that all pass (or fail to pass) threshold criteria. Our test of this possibility consisted of performing a voxel-wise ANOVA to test for session effects. Since we are trying to demonstrate the null hypothesis of no change, we chose to accept as significant a liberal $p<0.1$. Unsurprisingly, the results of the ANOVA analysis are in very good concordance with the correlation results. Figs. 2a and b use the same component numbering scheme, based on correlation value. Thus, it is readily apparent from Fig. 2b that the components with the highest correlation (toward the left of the graph) are those that also have the fewest voxels demonstrating a session effect. Furthermore, in particular, components in the PR1 group are among the most consistent. The pattern of these results is extremely similar for all thresholds used. The ANOVA was performed on the entire dataset, however the results were similar when we restricted the analysis to regions defined by the grand maps of Fig. 1 (results not shown). Taken together with the overlap results of Fig. 3, we have shown that not only is there consistency in space (i.e. the maps created by looking at each session), but there is consistency in functional value (i.e. the values that were used to define the space).

The consistency of the resting-state data over time is perhaps not surprising given the extensive literature looking at changes in activation using tasks. These changes have been investigated using both within- and between-subjects data. A variety of analytic tools have been employed, such as looking at the variability of between- and within-subjects with activation index (AI), defined by activated pixels, intraclass correlation coefficient (ICC), defined by the interaction ratio of within- and between-subject variance, or general linear statistical models (Aron et al., 2006; McGonigle et al., 2000; Smith et al., 2005; Wei et al., 2004). For example, studies have demonstrated consistent activation in the calcarine sulcus for a visual task (Rombouts et al., 1998), dorsolateral prefrontal cortex for an auditory 2-back working-memory task (Wei et al., 2004), primary auditory cortex in an auditory task (Yoo et al., 2005) and in frontostriatal regions in a probabilistic classification learning task (Aron et al., 2006). In contrast, others have shown learning or habituation to the task across sessions that have led to changes, even signal reversal, in primary sensorimotor regions in a passive motor task separated by 5 h or 1–2 months (Loubinoux et al., 2001) and in inferior parietal lobule in a visual search task across 5 consecutive days (Kubler et al., 2006). Single-subject studies over many sessions have shown that within-session variability is similar to between-session variability (Marshall et al., 2004; Smith et al., 2005). Taken together, these studies have shown that there are situations where there is repeatable session-to-session activation by tasks. Tasks likely tap into the networks observed in the resting-state data. For example, the 'default-mode' network in Fig. 1c is frequently seen deactivated during cognitive tasks (McKiernan et al., 2003) and the networks seen in Figs. 1e, f are frequently activated in cognitive tasks. Thus, stability of task-induced activation is likely a reflection of the stability of the underlying networks — networks that are observed in the resting-state.

One of the challenges of using ICA for fMRI analysis is component selection. When using ICA for analysis of task data, one typically chooses the components whose time-courses resemble the task design. However, this is not possible for the analysis of resting data. While our method, component review by neuroimaging experts, may appear arbitrary, it is consistent with the methods of others in the literature (Damoiseaux et al., 2006). This study has raised the possibility of an alternative selection criterion, or at least a guideline. The components chosen as the most physiologically recognizable had a statistically higher correlation than those chosen to be noise. Further, there was a trend for one of the less-certain groups (PR3) to be better correlated than noise as well. Thus, it

is possible that a ranking by consistency is a good starting point for component selection. In our study we have the luxury of five sessions of data to determine consistency, but it should be possible to use a bootstrap technique with a sufficiently large set of single-session data to compute a consistency metric for this use. The fact that the PR2 group had consistency measures no different than noise is somewhat disturbing. However, these components often contained a combination of anatomically reasonable regions and a small amount of unreasonable (e.g. out-of-brain or CSF) regions. This raises the possibility that these components were created by noise that correlated strongly with signal for a session, hence their lack of repeatability. Finally, it should be noted that, despite the PR1 components being statistically more consistent than the PR4 group, 4 of the 5 most consistent components came from PR4. However, these were among the easiest components to classify as PR4.

The majority of our components, 31 to 46 of the 55 total, appeared to be artifactual in nature. The component maps of a surprising 13 of these consisted primarily of eye 'activation'. It is likely that this was driven by the large motion the eyes can have coupled with associated spin-history and distortion effects. Several other components seemed to be concentrated in the brainstem, an area with known motion associated with cardiac pulsation (Dagli et al., 1999). The remainder of the artifactual components consisted of primarily ventricles/other CSF or obvious motion artifacts indicated by large amplitudes forming a ring around part of the brain. The consistency of these artifactual components may seem surprising. However, it is important to note that the analysis performed herein is based upon spatial ICA. This analysis will find similar spatial maps that do not necessarily have similar timecourses, neither across subjects nor across sessions. Thus, for example, head motion, eye motion or respiration changes that produce a given spatial pattern, but with different timecourses from scan-to-scan, will show up as a consistent component in our analysis. A possible solution to remove these components would be to mask these regions out of the analysis such that the analysis included only brain. Our primary motivation for including the regions outside the brain was to include voxels that would be putatively pure noise in the analysis, providing extra information about the noise structure that may help the ICA algorithm converge to an optimal solution. Anecdotally, we performed the analysis on voxels inside the brain only with results that seemed to converge to a less reasonable solution (i.e. many difficult to identify maps). Nonetheless, even with including out-of-cortex regions, our ratio of 'interesting' to noise components is consistent with others in the literature.

The gICA technique used in this manuscript apply and extend the work of Calhoun et al. (2001), who used two data reduction steps, within subject and following concatenation of subjects in the temporal direction. In the present work, each subject had five sessions of data, requiring an extension to the gICA procedure. We added an additional concatenation and reduction step at the session level; i.e. reduce within one session for one subject, concatenate within subject across sessions and reduce again, concatenate across subjects and final reduction. Thus we have a single set of components — that comprise our grand maps — created from the complete set of data. A different analysis approach would have been to perform separate gICA analysis for each session (or even separate ICA analyses for each scan) and compare consistency across analyses. However, there are two problems with this approach that would prevent the quantitative assessment of consistency that is necessary for longitudinal studies. The first problem is that of component matching. Our gICA approach was done as an effective means of avoiding the identification of similar components across 5 separate gICA decompositions. Although it is possible to make this identification in certain circumstances using, for example, clustering or correlation techniques (Damoiseaux et al., 2006), noise and number of components affect the ICA decomposition. These effects, for example, can split one component into two, making identification across sessions impossible for that component. The second, more critical, problem relates to the ICA procedure itself. ICA decomposes the data into the product of two unknown matrices. Thus the 'amplitude' of either matrix is indeterminate. That is, while it makes sense to compare the amplitudes within a column of one matrix (i.e. across space within a component) or within a row of the other (i.e. across time for the timecourse of a component), quantitative comparisons across components (or across different ICA analyses) are meaningless. Therefore it is important to note that the consistency comparisons performed in this manuscript were done in the context of this single, five-session gICA analysis. If the analyses were carried out separately for each session there would likely be greater variability between the identified physiologically recognizable components. However, separate analyses for each session were performed by Damoiseaux et al. (2006) with results strikingly similar to our own.

A limitation of this study is the duration over which the participants were scanned. These participants form a control group for a pharmacological manipulation study, hence the relatively short duration. It would be of obvious interest to establish the consistency of these networks over the course of months and years, durations useful for rehabilitation studies and other long-term disease or treatment manipulations. However, we have demonstrated the stability of these networks over a time useful for studying other phenomena such as acute medication or drug-withdrawal effects. Further, the number of studies using different cohorts and different methods resulting in similar patterns provides converging evidence that these networks are fundamental and likely stable over long durations. A second limitation of this study is that the TR used (2160 ms) is too long to critically sample, and thus permit filtering of, cardiac-induced fluctuations. This TR was selected as it permitted the high-resolution whole-brain scanning that is necessary to examine brain networks. Previous studies have shown that the resting-state connectivity obtained at short and moderate TRs are very similar (Biswal et al., 1995; Lowe et al., 1998). Furthermore, the spatial pattern of physiologically-driven noise should be independent from that of neuronally-driven networks and thus should appear in separate ICA components.

In conclusion, we have demonstrated what we believe are the most accurate representation to date, based upon the number of subjects and sessions, of brain networks defined by low-frequency fluctuations in the resting-state. Multiple analyses confirmed the stability of these networks over a 14 day timeframe.

4. Experimental procedures

4.1. Subjects

The studies were performed under a protocol approved by the Institutional Review Board at the National Institute on Drug Abuse. Signed informed consent was obtained from all participants. MRI experiments were performed on 14 healthy male right-handed volunteers (30±6 years old) who were serving as a timed control group in a larger study. The 5 scan sessions were scheduled to occur on days 2, 6, 7, 12 and 15 of the 16 day experiment. However, there was some variability in the scan days due to scheduling difficulties. The average time between first and last scan session was 14.9 days (range 12–24).

4.2. Scanning

Scanning was performed on a 3 T Siemens Allegra scanner (Erlangen, Germany). In each session, 90 whole-brain resting-state images (39 contiguous sagittal slices, 4 mm in thickness) were acquired using echo-planar imaging (EPI), with a 22×22 cm^2 field-of-view (FOV), 64×64 matrix (3.4×3.4 mm^2 in-plane resolution), 27 ms echo time (TE), 80° flip angle (FA) and 2160 ms repetition time (TR). There was no task performed during the scan; subjects were informed to rest and think of nothing in particular. The resting-state scan was performed about 10 min into a 90 min scan session consisting of cognitive and emotional tasks (presented elsewhere). Due to scanner failure, one subject missed data for session 1, one subject for sessions 2 and 3 and one subject from session 5. Missing data are handled well by the gICA procedure; however, these subjects were excluded from the ANOVA consistency analysis (described below). Additionally, a whole-brain T1 weighted anatomical image with isotropic resolution of 1 mm^3 was collected using the MPRAGE sequence (TR=2.5 s, TE=4.38 ms, FA=8°). This image was used for spatial normalization of the EPI images. Ear plugs were used to reduce acoustic noise, and foam packs were applied to restrict head motion.

4.3. Preprocessing

The resting-state EPI data were volume registered to correct for subject head motion, and temporally sinc-interpolated to correct for slice-timing effects. The data were then spatially normalized to Talairach space (Talairach and Tournoux, 1988) and resampled to $3\times3\times3$ mm^3. Finally, the images were spatially smoothed with a Gaussian kernel with full-width-at-half-maximum (FWHM) of 4 mm. The data were preprocessed in AFNI (Cox, 1996).

4.4. ICA

The data were analyzed using independent component analysis (ICA) (Bell and Sejnowski, 1995; McKeown et al., 1998). Briefly, ICA represents the data as a linear mixture of (spatially) independent sources. Given the data matrix $\mathbf{P}$ ($T\times V$, where T is the number of time points and V is the number of voxels), ICA seeks to represent $\mathbf{P}$ as the product of 2 matrices, $\mathbf{S}$ ($N\times V$, where $N\leq T$), the source matrix and $\mathbf{A}$ ($T\times N$), the mixing matrix; that is

$$\boldsymbol{P} = \mathbf{AS}.$$

The sources are approximated by finding an unmixing matrix $\mathbf{W}$ ($\mathbf{W}=\mathbf{A}^{-1}$) multiplied by the measured data, such that

$$\hat{\mathbf{S}} = \mathbf{W}\boldsymbol{P}.$$

The matrix $\mathbf{W}$ is chosen to make the sources as independent as possible (i.e. such that their joint probability factors, i.e. $P(a|b) = P(a)P(b)$). There are several algorithms to solve this problem; we used the FastICA approach (Hyvarinen, 1999).

4.5. Group ICA

Several approaches have been proposed to extend ICA to group analysis (see Schmithorst, 2004 for a comparison). We chose the method proposed by Calhoun et al. (2001) and Calhoun et al. (2004) where data are concatenated in the time direction. Group ICA was performed on the entire (14×5) data sets in two fashions. In the first group ICA (gICA$_1$), data sets were temporally concatenated through subjects and then sessions, similar to that proposed by Calhoun et al. for a single session. Principal component analysis (PCA) was used to reduce data dimensions in three steps: individual subject (30 components), concatenated through subjects (45 components), and concatenated through sessions (55 components). Dimensions of the fMRI data at the three levels were estimated using an improved method that utilizes a first-order auto-regressive (AR(1)) fitting technique to the PCA spectrum (Cordes and Nandy, 2006; Chen et al., 2007). Briefly, the difference from previous studies is that colored noise (i.e. AR(1) noise) was added into the group fMRI data prior to the final two reductions to blur the signal variation that contributes to the dimensional overestimation. In the second group ICA (gICA$_2$), data sets were temporally concatenated through sessions and then subjects. Similar to gICA$_1$, dimensions were estimated and PCA was used to reduce data dimensions at three steps: individual subject (35 components), concatenated through sessions (35 components), and concatenated through subjects (55 components). The average variance retained at each of these steps was 99.999%, 99.998% and 99.94% respectively. Grand maps of the independent components (ICs) were obtained from these two analyses on the entire data sets. Following the procedures similar to that of Calhoun et al. (2001), session-wise (individual sessions across subjects) and subject-wise (individual subjects across sessions) ICs were back-reconstructed from gICA$_2$ and gICA$_1$, respectively (see details in the Appendix). Similarly, ICs of individual subjects at individual sessions were obtained from the two grand analyses.

The gICA procedure produces a large set of results (in our case, 55 component maps). We applied a $z>3$ threshold, combined with a minimum cluster extent of 200 μl, to each component map. For reporting purposes, component maps were subjectively separated using our knowledge of the cognitive-neuroscience literature into four groups based upon the physiological recognizability (PR) of the map, henceforth referred to as PR1–PR4. Examples of a PR1 map,

i.e. maps that we were maximally confident to represent meaningful physiological processes, are bilateral motor cortex or bilateral auditory cortex, whereas a PR4 map, i.e. maps we believe to be artifact-driven, are ventricles/CSF, eyes or edge-of-brain indicative of head motion. PR1 maps are shown in the results section — the other groups in the Supplemental material. Sorting according to PR occurred before consistency analysis, which was performed on all groups.

4.6. *Consistency analysis*

The consistency of the gICA maps across sessions was assessed using 3 different approaches. First, we back-reconstructed the five single-session maps for each component. Pearson's correlation components were calculated between each session map and the grand map and averaged over the sessions as a consistency indication. In order to determine if the component maps that appear the most physiologically recognizable are the most consistent, the average correlations were compared between the 4 groups with a Kruskal–Wallis test followed by Mann–Whitney post-hoc tests as appropriate (Statview, SAS Institute, Cary NC).

Next, we investigated the question of the consistency from a mapping point of view using a conjunction analysis. Again, we back-projected the data to create individual session maps. The same threshold was applied to these maps as the grand map ($z>3$, minimum of 200 μl). Consistent voxels were defined as those that passed threshold in all 5 sessions. We additionally show voxels active in at least 3 of the 5 sessions.

This second method is analogous to voxel-counting analysis in that we are determining whether voxels passed threshold in both data sets (in our case a given session and the grand map). This type of analysis can be misleading in that a region may appear in one group and not the other, thus implying a difference that is not supported by a direct statistical analysis between the groups in that region. To address this, and to investigate stability from an inconsistency point of view, voxel-wise ANOVA was performed as the final method. The data were back-projected to the first (individual subject) level. For each component map, 2-way ANOVA (session and subject as factors) was executed on each voxel, with fraction of voxels with no session effect as the consistency measure. As we are essentially trying to demonstrate the null hypothesis, a threshold as liberal as $p<0.1$ was applied to the ANOVA results.

Acknowledgments

This work was supported by the Intramural Research Program of the NIH, National Institute on Drug Abuse.

Appendix A

A.1 Concatenation and reduction in gICA

A series of fMRI images ($\mathbf{Y}$) were collected from N subjects with T time points each in M sessions. The image size for one subject per session is TV, where V is the volume size. Each 3D+Time image was preprocessed and spatially normalized into Talairach space. At the first level, each single-session data was generated from concatenating the single-subject data that was reduced using PCA. Hence, the first level concatenated data ($\mathbf{X}$) is given by:

$$\mathbf{X} = \begin{bmatrix} \mathbf{F}_1^{-1}\mathbf{Y}_1 \\ \vdots \\ \mathbf{F}_N^{-1}\mathbf{Y}_N \end{bmatrix} \tag{a1}$$

Where $\mathbf{F}_i^{-1}$ is the reducing matrix (K-by-T, $K \le T$) for the i^{th} subject.

Eq. (a1) is repeated at the session level across sessions, yielding the session concatenated data at the second level. The equation for this reduction and concatenation is:

$$\mathbf{O} = \begin{bmatrix} \mathbf{G}_1^{-1}\mathbf{X}_1 \\ \vdots \\ \mathbf{G}_M^{-1}\mathbf{X}_M \end{bmatrix} \tag{a2}$$

Where $\mathbf{G}_j^{-1}$ is the reducing matrix (L-by-KN, $L \le KN$) for the j^{th} session. The data concatenated across session is reduced once more:

$$\boldsymbol{P} = \mathbf{H}^{-1}\mathbf{O} \tag{a3}$$

Where $\mathbf{H}^{-1}$ is the reducing matrix (U-by-LM, $U \le LM$) for the group data. K, L and U represent the reduction number at each level and determined by an improved AR(1) fitting to the eigenvalue spectrum (Cordes and Nandy, 2006; Chen et al., 2007).

The independent components ($\mathbf{S}$) are approximated from $\boldsymbol{P}$ by finding an unmixing matrix ($\mathbf{W}$), namely $\hat{\mathbf{S}}=\mathbf{W}\boldsymbol{P}$. This is from the ICA basic assumption, that the observed data can be regarded as a linear combination of statistically independent components, namely $\boldsymbol{P}=\mathbf{AS}$. Thus, the session concatenated data can be obtained from

$$\mathbf{HAS} = \mathbf{O} \tag{a4}$$

The matrix can be partitioned into:

$$\begin{bmatrix} \mathbf{H}_1 \\ \vdots \\ \mathbf{H}_M \end{bmatrix} \mathbf{AS} = \begin{bmatrix} \mathbf{G}_1^{-1}\mathbf{X}_1 \\ \vdots \\ \mathbf{G}_M^{-1}\mathbf{X}_M \end{bmatrix} \tag{a5}$$

The matrices $\mathbf{A}$ and $\mathbf{S}$ are estimate using ICA.

A.2 Backward reconstruction from the gICA results

Given the estimations for $\mathbf{A}$ and $\mathbf{S}$ and the reducing matrices, projections for single sessions can be calculated. For the j^{th} session, partition the equation is:

$$\mathbf{X}_j = \mathbf{G}_j\mathbf{H}_j\hat{\mathbf{A}}\hat{\mathbf{S}}_j \tag{a6}$$

Similarly, for the i^{th} subject during the j^{th} session the equation is:

$$\mathbf{Y}_{ji} = \left(\mathbf{G}_{ji}\mathbf{F}_{ji}\right)\left(\mathbf{H}\hat{\mathbf{A}}\right)_j\hat{\mathbf{S}}_{ji} \tag{a7}$$

where $\left(\mathbf{G}_{ji}\mathbf{F}_{ji}\right)\left(\mathbf{H}\hat{\mathbf{A}}\right)_j$ is the component time course for the i^{th} subject during the j^{th} session.

Appendix A. Supplementary data

Supplementary data associated with this article can be found, in the online version, at doi:10.1016/j.brainres.2008.08.028.

REFERENCES

Anand, A., Li, Y., Wang, Y., Wu, J., Gao, S., Bukhari, L., Mathews, V.P., Kalnin, A., Lowe, M.J., 2005. Antidepressant effect on connectivity of the mood-regulating circuit: an FMRI study. Neuropsychopharmacology 30, 1334–1344.

Aron, A.R., Gluck, M.A., Poldrack, R.A., 2006. Long-term test–retest reliability of functional MRI in a classification learning task. Neuroimage 29, 1000–1006.

Beckmann, C.F., DeLuca, M., Devlin, J.T., Smith, S.M., 2005. Investigations into resting-state connectivity using independent component analysis. Philos. Trans. R. Soc. Lond. B. Biol. Sci. 360, 1001–1013.

Bell, A.J., Sejnowski, T.J., 1995. An information maximization approach to blind separation and blind deconvolution. Neural Comput. 7, 1129–1159.

Biswal, B., Yetkin, F.Z., Haughton, V.M., Hyde, J.S., 1995. Functional connectivity in the motor cortex of resting human brain using echo-planar MRI. Magn. Reson. Med. 34, 537–541.

Boly, M., Phillips, C., Tshibanda, L., Vanhaudenhuyse, A., Schabus, M., Dang-Vu, T.T., Moonen, G., Hustinx, R., Maquet, P., Laureys, S., 2008. Intrinsic brain activity in altered states of consciousness: how conscious is the default mode of brain function? Ann. N. Y. Acad. Sci. 1129, 119–129.

Calhoun, V.D., Adali, T., Pearlson, G.D., Pekar, J.J., 2001. A method for making group inferences from functional MRI data using independent component analysis. Hum. Brain Mapp. 14, 140–151.

Calhoun, V.D., Adali, T., Pekar, J.J., 2004. A method for comparing group fMRI data using independent component analysis: application to visual, motor and visuomotor tasks. Magn. Reson. Imaging 22, 1181–1191.

Chen, S., Ross, T.J., Chuang, K.-S., Stein, E.A., Yang, Y., Zhan, W., 2007. Dimensionality Estimation for Group fMRI Data Reduction at Multiple Levels. SPIE Symposium on Medical Imaging. San Diego, CA, pp. 6511–6541.

Comon, P., 1994. Independent component analysis, a new concept. Signal Process. 36, 287–314.

Cordes, D., Nandy, R.R., 2006. Estimation of the intrinsic dimensionality of fMRI data. Neuroimage 29, 145–154.

Cordes, D., Haughton, V.M., Arfanakis, K., Wendt, G.J., Turski, P.A., Moritz, C.H., Quigley, M.A., Meyerand, M.E., 2000. Mapping functionally related regions of brain with functional connectivity MR imaging. AJNR Am. J. Neuroradiol. 21, 1636–1644.

Cox, R.W., 1996. AFNI: software for analysis and visualization of functional magnetic resonance neuroimages. Comput. Biomed. Res. 29, 162–173.

Dagli, M.S., Ingeholm, J.E., Haxby, J.V., 1999. Localization of cardiac-induced signal change in fMRI. Neuroimage 9, 407–415.

Damoiseaux, J.S., Rombouts, S.A., Barkhof, F., Scheltens, P., Stam, C.J., Smith, S.M., Beckmann, C.F., 2006. Consistent resting-state networks across healthy subjects. Proc. Natl. Acad. Sci. U. S. A. 103, 13848–13853.

Fox, M.D., Snyder, A.Z., Vincent, J.L., Corbetta, M., Van Essen, D.C., Raichle, M.E., 2005. The human brain is intrinsically organized into dynamic, anticorrelated functional networks. Proc. Natl. Acad. Sci. U. S. A. 102, 9673–9678.

Fukunaga, M., Horovitz, S.G., van Gelderen, P., de Zwart, J.A., Jansma, J.M., Ikonomidou, V.N., Chu, R., Deckers, R.H., Leopold, D.A., Duyn, J.H., 2006. Large-amplitude, spatially correlated fluctuations in BOLD fMRI signals during extended rest and early sleep stages. Magn. Reson. Imaging 24, 979–992.

Greicius, M.D., Krasnow, B., Reiss, A.L., Menon, V., 2003. Functional connectivity in the resting brain: a network analysis of the default mode hypothesis. Proc. Natl. Acad. Sci. U. S. A. 100, 253–258.

Gusnard, D.A., Raichle, M.E., 2001. Searching for a baseline: functional imaging and the resting human brain. Nat. Rev. Neurosci. 2, 685–694.

Hyvarinen, A., 1999. Fast and robust fixed-point algorithms for independent component analysis. IEEE Trans. Neural Netw. 10, 626–634.

Kubler, A., Dixon, V., Garavan, H., 2006. Automaticity and reestablishment of executive control-an fMRI study. J. Cogn. Neurosci. 18, 1331–1342.

Li, S.J., Li, Z., Wu, G., Zhang, M.J., Franczak, M., Antuono, P.G., 2002. Alzheimer Disease: evaluation of a functional MR imaging index as a marker. Radiology 225, 253–259.

Liang, M., Zhou, Y., Jiang, T., Liu, Z., Tian, L., Liu, H., Hao, Y., 2006. Widespread functional disconnectivity in schizophrenia with resting-state functional magnetic resonance imaging. Neuroreport 17, 209–213.

Loubinoux, I., Carel, C., Alary, F., Boulanouar, K., Viallard, G., Manelfe, C., Rascol, O., Celsis, P., Chollet, F., 2001. Within-session and between-session reproducibility of cerebral sensorimotor activation: a test–retest effect evidenced with functional magnetic resonance imaging. J. Cereb. Blood Flow Metab. 21, 592–607.

Lowe, M.J., Mock, B.J., Sorenson, J.A., 1998. Functional connectivity in single and multislice echoplanar imaging using resting-state fluctuations. Neuroimage 7, 119–132.

Marshall, I., Simonotto, E., Deary, I.J., Maclullich, A., Ebmeier, K.P., Rose, E.J., Wardlaw, J.M., Goddard, N., Chappell, F.M., 2004. Repeatability of motor and working-memory tasks in healthy older volunteers: assessment at functional MR imaging. Radiology 233, 868–877.

McGonigle, D.J., Howseman, A.M., Athwal, B.S., Friston, K.J., Frackowiak, R.S., Holmes, A.P., 2000. Variability in fMRI: an examination of intersession differences. Neuroimage 11, 708–734.

McKeown, M.J., Makeig, S., Brown, G.G., Jung, T.P., Kindermann, S.S., Bell, A.J., Sejnowski, T.J., 1998. Analysis of fMRI data by blind separation into independent spatial components. Hum. Brain Mapp. 6, 160–188.

McKiernan, K.A., Kaufman, J.N., Kucera-Thompson, J., Binder, J.R., 2003. A parametric manipulation of factors affecting task-induced deactivation in functional neuroimaging. J. Cogn. Neurosci. 15, 394–408.

Raichle, M.E., Gusnard, D.A., 2005. Intrinsic brain activity sets the stage for expression of motivated behavior. J. Comp. Neurol. 493, 167–176.

Raichle, M.E., MacLeod, A.M., Snyder, A.Z., Powers, W.J., Gusnard, D.A., Shulman, G.L., 2001. A default mode of brain function. Proc. Natl. Acad. Sci. U. S. A. 98, 676–682.

Raz, A., Buhle, J., 2006. Typologies of attentional networks. Nat. Rev. Neurosci. 7, 367–379.

Rombouts, S.A., Barkhof, F., Hoogenraad, F.G., Sprenger, M., Scheltens, P., 1998. Within-subject reproducibility of visual activation patterns with functional magnetic resonance imaging using multislice echo planar imaging. Magn. Reson. Imaging 16, 105–113.

Schmithorst, V.J., 2004. Comparison of three methods for generating group statistical inferences from independent component analysis of functional magnetic resonance imaging data. J. Magn. Reson. Imaging 19, 365–368.

Shulman, R.G., Rothman, D.L., Behar, K.L., Hyder, F., 2004. Energetic basis of brain activity: implications for neuroimaging. Trends Neurosci. 27, 489–495.

Sibson, N.R., Dhankhar, A., Mason, G.F., Rothman, D.L., Behar, K.L., Shulman, R.G., 1998. Stoichiometric coupling of brain glucose metabolism and glutamatergic neuronal activity. Proc. Natl. Acad. Sci. U. S. A. 95, 316–321.

Smith, S.M., Beckmann, C.F., Ramnani, N., Woolrich, M.W., Bannister, P.R., Jenkinson, M., Matthews, P.M., McGonigle, D.J., 2005. Variability in fMRI: a re-examination of inter-session differences. Hum. Brain Mapp. 24, 248–257.

Talairach, J., Tournoux, P., 1988. Co-planar Stereotaxic Atlas of the Human Brain. Thieme, New York.

van de Ven, V.G., Formisano, E., Prvulovic, D., Roeder, C.H., Linden, D.E.J., 2004. Functional connectivity as revealed by spatial independent component analysis of fMRI measurements during rest. Hum. Brain Mapp. 22, 165–178.

Waites, A.B., Briellmann, R.S., Saling, M.M., Abbott, D.F., Jackson, G.D., 2006. Functional connectivity networks are disrupted in left temporal lobe epilepsy. Ann. Neurol. 59, 335–343.

Waites, A.B., Stanislavsky, A., Abbott, D.F., Jackson, G.D., 2005. Effect of prior cognitive state on resting state networks measured with functional connectivity. Hum. Brain Mapp. 24, 59–68.

Wei, X., Yoo, S.S., Dickey, C.C., Zou, K.H., Guttmann, C.R., Panych, L.P., 2004. Functional MRI of auditory verbal working memory: long-term reproducibility analysis. Neuroimage 21, 1000–1008.

Xiong, J., Parsons, L.M., Gao, J.H., Fox, P.T., 1999. Interregional connectivity to primary motor cortex revealed using MRI resting state images. Hum. Brain Mapp. 8, 151–156.

Yoo, S.S., O'leary, H.M., Dickey, C.C., Wei, X.C., Guttmann, C.R., Park, H.W., Panych, L.P., 2005. Functional asymmetry in human primary auditory cortex: identified from longitudinal fMRI study. Neurosci. Lett. 383, 1–6.